Inactivation of Kv2.1 Potassium Channels

Kathryn G. Klemic,* Char-Chang Shieh,*# Glenn E. Kirsch,*# and Stephen W. Jones*

*Department of Physiology and Biophysics, Case Western Reserve University, Cleveland, Ohio 44106, and #Rammelkamp Center for Research, MetroHealth Medical Center, Cleveland, Ohio 44109 USA

ABSTRACT   We report here several unusual features of inactivation of the rat Kv2.1 delayed rectifier potassium channel, expressed in *Xenopus* oocytes. The voltage dependence of inactivation was U-shaped, with maximum inactivation near 0 mV. During a maintained depolarization, development of inactivation was slow and only weakly voltage dependent ($\tau = 4$ s at 0 mV; $\tau = 7$ s at $+80$ mV). However, recovery from inactivation was strongly voltage dependent (e-fold for 20 mV) and could be rapid ($\tau = 0.27$ s at -140 mV). Kv2.1 showed cumulative inactivation, where inactivation built up during a train of brief depolarizations. A single maintained depolarization produced more steady-state inactivation than a train of pulses, but there could actually be more inactivation with the repeated pulses during the first few seconds. We term this phenomenon "excessive cumulative inactivation." These results can be explained by an allosteric model, in which inactivation is favored by activation of voltage sensors, but the open state of the channel is resistant to inactivation.

INTRODUCTION

Kv2.1 (drk1; Frech et al., 1989) is a voltage-dependent potassium channel related to the *Shab* channel of *Drosophila*. It is expressed in a wide variety of excitable cells, including central (Trimmer, 1993) and peripheral (Dixon and McKinnon, 1996) neurons, as well as cardiac (Dixon and McKinnon, 1994; Barry et al., 1995; Brahmajothi et al., 1996) and skeletal (Drewe et al., 1992) muscle. Its precise physiological function has not been established, but when expressed in heterologous systems, its biophysical characteristics closely match those of delayed rectifier currents, which are involved in repolarization of the action potential in many excitable membranes. A characteristic feature of delayed rectification, as exemplified by Kv2.1, is that brief depolarization activates the channel, but sustained depolarization causes a slow inactivation (VanDongen et al., 1990). Such slow inactivation is seen for many cloned potassium channels of the Kv superfamily, and is generally termed "C-type" inactivation (Hoshi et al., 1991), to contrast with "N-type" inactivation by the "ball-and-chain" mechanism (Hoshi et al., 1990). In Kv1-class channels, C-type inactivation is thought to involve a concerted constriction of the outer part of the channel pore (Ogielska et al., 1995; Panyi et al., 1995; Liu et al., 1996). Onset of C-type inactivation is slowed by extracellular tetraethylammonium (TEA) and by high K_o^+ (Grissmer and Cahalan, 1989; DeCoursey, 1990; Choi et al., 1991; Levy and Deutsch, 1996; Baukrowitz and Yellen, 1996).

The slow kinetics of delayed rectifier inactivation during a maintained depolarization might suggest that inactivation is physiologically irrelevant, at least for typical brief neuronal action potentials. However, several native or cloned delayed rectifiers show cumulative inactivation, where inactivation builds up during a train of brief depolarizations (Aldrich et al., 1979a; DeCoursey et al., 1984; Matteson and Deutsch, 1984; Marom et al., 1993; Quattrocki et al., 1994; Mathes et al., 1997). Several models have been proposed for cumulative inactivation, generally incorporating the idea that inactivation is state-dependent, rather than depending directly on membrane potential (Aldrich, 1981; DeCoursey, 1990; Marom and Levitan, 1994).

The work reported here actually began as a study of activation kinetics of the Kv2.1 potassium channel (Klemic et al., 1997). We chose that channel in part because of its slow inactivation, which should have allowed study of the activation process in isolation. However, even brief depolarizations, where the current showed no visible inactivation, reduced the current evoked by a subsequent depolarization. That observation, reminiscent of cumulative inactivation, led us to examine the kinetics of inactivation more closely. We found two especially surprising results. First, the dependence of inactivation on voltage was not monotonic, but U-shaped, with less inactivation at strong depolarizations. Second, the channel exhibited excessive cumulative inactivation, where for some conditions, a train of depolarizations could produce more inactivation than a single step of the same duration. Both results can be simply explained if the channel inactivates preferentially from "partially activated" closed states. We propose a kinetic model in which inactivation from closed states is allosterically coupled to voltage sensor movement (Jones, 1992; Kuo and Bean, 1994), with little inactivation from the open state of the channel.

MATERIALS AND METHODS

Molecular biology and oocyte injection

Kv2.1 was expressed in *Xenopus* oocytes as previously described (Shieh et al., 1997). In short, the Kv2.1 clone (Frech et al., 1989) was propagated in

---

Address reprint requests to Dr. Kathryn G. Klemic, Department of Physiology and Biophysics, Case Western Reserve University, Cleveland, OH 44106. Tel.: 216-368-5526; Fax: 216-368-3952; E-mail: kxg13@po.cwru.edu

the transcription-competent plasmid vector pBluescript SK(−). Capped cRNA runoff transcripts were prepared from *Not*I-linearized cDNA using T7 RNA polymerase. Stage V or VI *Xenopus* oocytes were defoliculated enzymatically, injected with 46 nl of cRNA solution at a concentration of 0.3–1 pg/nl (whole cell) or 250 pg/nl (macropatch), and used for recording 2–6 days after injection.

Voltage clamp

Whole-cell currents were recorded with a two-microelectrode voltage clamp as previously described (Drewe et al., 1994). Briefly, sharp-tipped agarose-cushion micropipettes (0.2–0.5 MΩ; Schreibmayer et al., 1994) were used as voltage-sensing and current-passing electrodes, with a commercial voltage-clamp amplifier (OC725C; Warner Instruments, Hamden, CT). Steady-state current levels during a series of hyperpolarizing pulses, −140 to −95 mV for 180 ms, were used to calculate the leak conductance. The calculated linear leakage current was digitally subtracted offline for all current measurements. The records shown in Figs. 2–4 were not leak- or capacitance-subtracted, but the holding current was subtracted, and a brief period (1–1.5 ms) was blanked during capacitative transients.

Cell-attached macropatch currents were recorded from devitellinized oocytes, with Sylgard-coated pipettes. Currents were sampled at 10 kHz after 2-kHz analog filtering with an Axopatch 1C amplifier (Axon Instruments, Foster City, CA). Linear leakage and capacitative transient currents were digitally subtracted with a P/4 subtraction routine. All voltage steps were recorded from a holding potential of −90 mV.

Solutions

The standard extracellular solution, used for two-electrode voltage clamp and to fill the pipette for cell-attached recording, was (in mM) 117.5 *N*-methyl-ᴅ-glucamine (NMG) methane sulfonic acid (MES), 5 KCl, 4 CaCl₂, and 10 HEPES, adjusted to pH 7.3 with NMG base. Where noted, KCl was increased to 60 mM, with KCl replacing NMG-MES. Some experiments used a modified frog Ringer's containing (in mM) 120 NaCl, 1 CaCl₂, 2 MgCl₂, 10 HEPES, pH 7.2 with Tris-OH, or a 120 mM K⁺

solution with KCl replacing NaCl. For cell-attached recording, the oocyte was bathed in a depolarizing solution (in mM): 100 KCl, 10 EGTA, 10 HEPES, pH 7.3 with KOH.

Data analysis

Data were recorded and analyzed with pClamp software (v. 5.6 or v. 6). The solver function of Microsoft Excel (v. 5.0) was used for single exponential fits to the time course of cumulative inactivation and of recovery from inactivation. Unless noted otherwise, values are expressed as mean ± SEM.

Kinetic models

Model data were simulated using the SCoP simulation package (v. 3.4; Simulation Resources, Berrien Springs, MI). Simulation results were imported into Excel for further analysis.

RESULTS

Inactivation of Kv2.1 has a U-shaped voltage dependence

In the course of studying the activation kinetics of the rat Kv2.1 potassium channel in cell-attached macropatches on *Xenopus* oocytes, we observed that the current tended to vary during repeated depolarizations, possibly reflecting inactivation or rundown. That phenomenon was particularly evident with the three-pulse protocol shown in Fig. 1 *A*. That protocol was designed to examine both activation (in the first step of each sequence, P1) and deactivation (in the tail currents, P3). Although the middle (P2) steps were to
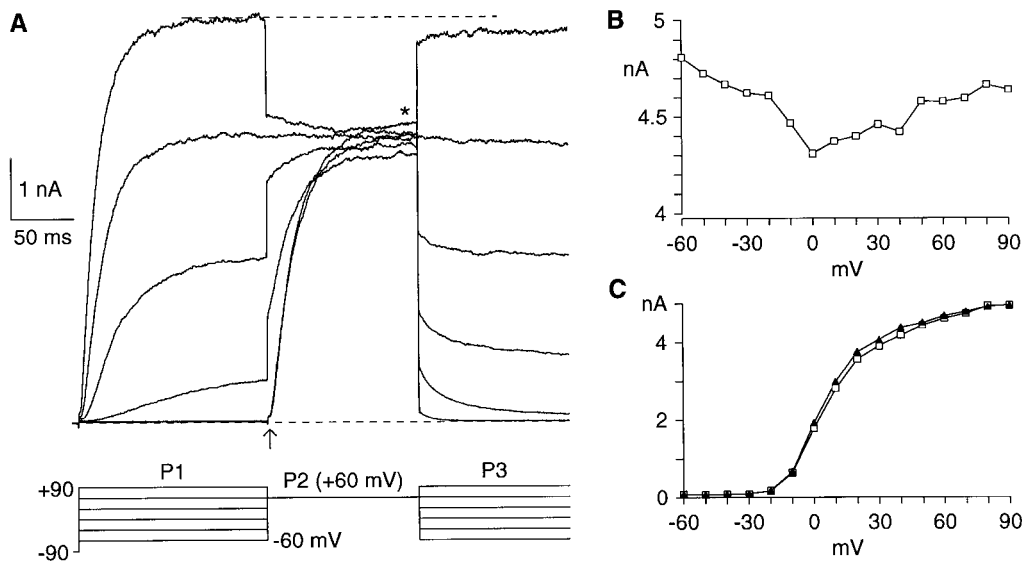

FIGURE 1 Inactivation of Kv2.1 by brief depolarization in cell-attached macropatches. (*A*) Currents elicited by depolarizations in 30-mV increments. For each record, the voltage was the same for P1 and P3, and P2 was to +60 mV. (*B*) Inactivation produced by a 150-ms P1. Currents, I2(end), were measured at the end of P2 (*asterisk in A*), and are shown as a function of the P1 voltage. (*C*) The activation curve, measured from the initial current during P2 (at 0.4–1.4 ms, see the *arrow in A*). Values are raw current measurements (□), or were corrected for inactivation (▲). The corrected values were calculated by dividing by I2(end), and then multiplying by the I2(end) for the record with a P1 of +90 mV. These P1 pulses were not long enough to reach true steady-state activation (note that the final P1 and P3 current levels in *A* are different, at −30 and 0 mV).

the same voltage in each case ($+60$ mV), the current at the end of that step was variable. Strikingly, the current did not simply decrease from step to step, but was the smallest after steps to intermediate voltages, producing a U-shaped voltage dependence (Fig. 1 *B*). The decrease in current occurred in the voltage range in which channels were partly activated, as shown by the activation curve measured from the currents at the start of P2 (Fig. 1 *C*, *open squares*). If we assume that the current at the end of P2 reflects the number of available channels, the "corrected" activation curve is slightly steeper (Fig. 1 *C*, *closed triangles*). These changes in current could interfere with detailed analysis of activation kinetics.

It is also apparent from Fig. 1 *A* that the current at $+90$ mV decreased from P1 to P3 (*dashed line*). The decrease in current during closely spaced voltage steps suggested cumulative inactivation.

Because highly stable recordings were necessary to study a process as slow as K$^+$ channel inactivation, we recorded currents from oocytes with a two-electrode voltage clamp. We began by examining inactivation produced by long, maintained depolarizations (Fig. 2). Inactivation is measured most simply as the decay in current during a depolarization (i.e., the current at the end of the pulse divided by the peak current). That measure could be misleading, because cumulative inactivation can occur even if there is no decrease in current during a depolarization. Instead, we used a variant of the classic two-pulse protocol used to examine inactivation of calcium channels (Tillotson, 1979). We added a brief prepulse (P1) to $+80$ mV at the beginning of each record, as a control for accumulation of inactivation during the protocol, and to allow measurement of inactivation as the ratio of the currents at $+80$ mV (I3/I1, Fig. 2, *A* and *B*). For a P2 lasting 1.2 s, there was a clear U-shaped voltage dependence for both measures of inactivation (Fig. 2 *C*). However, the I3/I1 ratio indicated that more inactivation had occurred than was visible during P2. For a longer P2 (19 s), inactivation was stronger (Fig. 2 *B*) and still exhibited a U shape. The fraction of current remaining after a 19-s step was 0.10 ± 0.02 at 0 mV, compared to 0.23 ± 0.04 at $+80$ mV (I3/I1 ratios, $n = 5$).

Other features of the inactivation process are revealed by close examination of the data. First, comparing the three depolarizations to $+80$ mV in Fig. 2 *A*, the current decreased from pulse to pulse, with the peak current in P2 and P3 smaller than the current at the end of the preceding pulse (*dashed lines*). Second, significant inactivation was produced by weak depolarizations that open few channels. After 19-s depolarizations, the $V_{1/2}$ for inactivation was -26 mV, with a slope of *e*-fold for 6.7 mV, fitting data up to $+20$ mV to a Boltzmann relation. Those values are comparable to previous results for Kv2.1, measured over a comparable voltage range, with 10–30-s pulses (VanDongen et al., 1990; Ikeda et al., 1992; Shi et al., 1994). For comparison, the $V_{1/2}$ for activation is near 0 mV (VanDongen et al., 1990; Ikeda et al., 1992; Shi et al., 1994; Shieh et al., 1997;
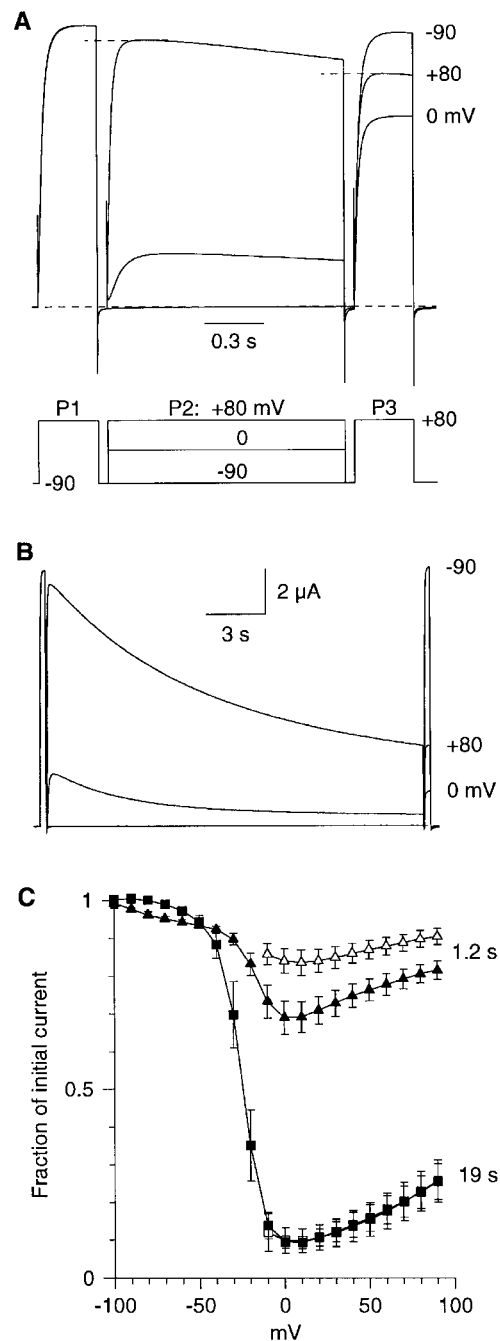

FIGURE 2 Inactivation has a U-shaped voltage dependence. (*A*) Currents recorded using a two-electrode voltage clamp, for the voltage protocol shown below. P1 and P3 were to $+80$ mV for 0.3 s, with P2 to -100, 0, or $+80$ mV for 1.2 s. The P2 voltage is shown to the right of the P3 record. The dashed lines emphasize the cumulative inactivation at $+80$ mV. (*B*) Inactivation with longer (19 s) P2 pulses. The protocol was otherwise as in *A*. In *A* and *B*, each record was normalized to the peak P1 current, which varied from 12.3 to 7.9 μA. (*C*) The voltage dependence of inactivation. Data were recorded using the protocol of *A*, for P2 of 1.2 or 19 s. Inactivation was measured either from the I3/I1 ratio ($\blacktriangle$, $\blacksquare$), or from the I2(end)/I2(peak) ratio ($\triangle$, $\square$). Values are mean $\pm$ SD ($n = 5$). At more negative voltages (-90 to -60 mV), there was more inactivation after 1.2-s pulses than after 19 s, probably reflecting inactivation during P1 ($\sim$5%) that did not fully recover during the 1.2-s P2.

see also Fig. 1 *C*), and the $V_{1/2}$ for gating charge movement is −22 mV (Shieh et al., 1997).

For calcium channels, a U-shaped inactivation curve is often taken as evidence for current-dependent inactivation (Eckert and Chad, 1984). That is not the case here. First, for a K⁺ current, the driving force continues to increase with depolarization, so current-dependent inactivation would actually increase monotonically with voltage. Second, the U shape was also seen in 60 mM K_o^+ (data not shown), where the reversal potential was near −10 mV. In that condition, inactivation was strong near the reversal potential, where there is neither net influx nor net efflux of K⁺. Finally, the U-shaped dependence of inactivation on voltage was observed in oocytes expressing widely varying levels of Kv2.1 channels, with outward currents at +80 mV ranging from 5 to 20 μA. These results also rule out the possibility that inactivation is an artifact of extracellular K⁺ accumulation.

Recovery from inactivation is strongly voltage-dependent

We measured recovery from inactivation with the protocol shown in Fig. 3 *A*. After a brief P1 to +80 mV, inactivation was produced by a long (5 or 12 s) P2 to 0 mV. Channels were then allowed to recover for a variable duration (20 ms to 40 s) at voltages ranging from −40 to −140 mV. Because of the wide range of recovery times and recovery rates, a logarithmic time scale is used in Fig. 3 *B*. Recovery from inactivation was well described by a single exponential (Fig. 3 *B*) and was strongly voltage-dependent (Fig. 3 *C*), changing *e*-fold for 20 mV from −120 mV to −40 mV. For comparison, the time constants for inactivation are also shown (Fig. 3 *C*, *triangles*), measured from 19-s depolarizations (from the experiments of Fig. 2 *B*). Development of inactivation was only weakly voltage-dependent, with a U

shape, with faster inactivation near 0 mV than at more negative or positive voltages. Recovery from inactivation could be >10-fold faster than development of inactivation.

In the middle of the voltage range, both inactivation and recovery were extremely slow. At −40 mV, little inactivation occurred during 19-s depolarizations (~10%, Fig. 2 *B*), but there was also only partial recovery over 40 s (~30%, Fig. 3 *B*). At steady-state inactivation, defined as the point at which inactivation and recovery from inactivation protocols converge (using protocols lasting up to 600 s), 39.5 ± 0.04% of the channels were inactivated at −40 mV (*n* = 5). This slow time course means that inactivation measured at 19 s (Fig. 2 *C*) is not a true steady-state inactivation curve.

Inactivation and recovery were also examined in 60 mM K_o^+ (Fig. 3 *C*, *open symbols*). The time constants for recovery were approximately twofold faster in 60 mM K_o^+, with no change in the shape of the voltage dependence. The time constant for onset of inactivation was slightly faster in 60 mM K_o^+ (Fig. 3 *C*), in contrast to results for Kv1 channels (López-Barneo et al., 1993; Levy and Deutsch, 1996). During 16-s pulses to +40 mV, the time constant for inactivation was 5.2 ± 0.1 s (*n* = 7) in normal Ringer's (2.4 mM K_o^+), and 3.0 ± 0.1 s (*n* = 4) in 120 mM K_o^+. Another difference from C-type inactivation of Kv1-class channels is that extracellular TEA did not slow inactivation of Kv2.1. In the presence of 5 mM TEA, which blocked 50% of the peak current, the time constant for inactivation in normal Ringer's at +40 mV was 4.5 ± 0.2 s (*n* = 3).

Excessive cumulative inactivation

Because inactivation occurs even with short depolarizations, repeated short pulses should produce cumulative inactivation. Not only does inactivation accumulate with repeated pulses, inactivation during a train can be faster than

FIGURE 3 Recovery from inactivation. (*A*) The protocol used to examine recovery from inactivation, shown for a recovery voltage of −90 mV. P1 and P3 were to +80 mV, and P2 to 0 mV, in each record. The data were normalized to the peak P1 current. (*B*) The time course of recovery from inactivation. The I3/I1 ratio is shown as a function of time, on a logarithmic time scale. P2 was to 0 mV, and lasted either 5 s (for recovery voltages of −140 to −90 mV) or 12 s (for −60 and −40 mV). The recovery voltages are given near the data points, except for −120 mV (△). Values are means (*n* = 3–7). (*C*) Time constants for inactivation (at −20 to +90 mV, △, ▲) and recovery from inactivation (−140 to −40 mV, □, ■) on a semilogarithmic scale. Data were recorded with 5 mM K_o^+ (▲, ■) or 60 mM K_o^+ (△, □). Values are means (*n* = 3–7, except *n* = 2 for 60 mM K_o^+ at −20, −40, and −60 mV).
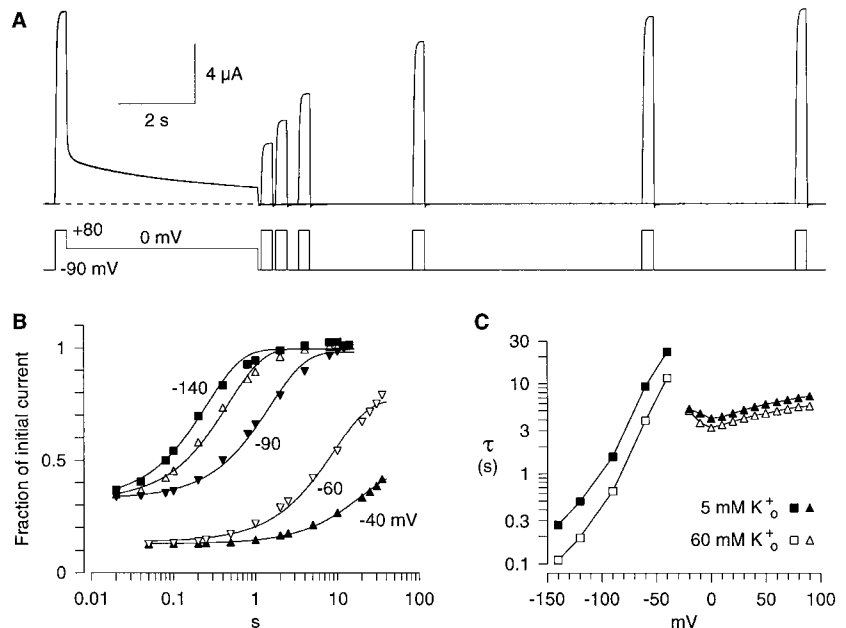
inactivation during a single maintained pulse of the same duration (Fig. 4 *A*). In the example shown, the time constant for inactivation was 2.5 s for repeated pulses versus 8 s for the maintained pulse. The difference in inactivation rate was clearest for strong depolarizations (e.g., +80 mV). There was little difference between the time constants for inactivation for pulses versus trains to 0 mV (data not shown). When the pulse duration was varied from 20 to 300 ms, keeping the duty cycle constant at 2:1, inactivation was slower and less complete during trains of longer pulses, at the times tested (Fig. 4, *B* and *C*).

To further examine the effect of pulse length on inactivation, we gave trains in which a total of 1 s was spent at the depolarized voltage, with pulse lengths ranging from 2 ms to 1000 ms, and interpulse intervals of 50 ms at −90 mV (Fig. 5). For depolarizations to 0 mV, the amount of inactivation increased monotonically with pulse length. However, at +80 mV, inactivation was at maximum for intermediate pulse lengths (∼20 ms).

In these experiments, the final level of cumulative inactivation was less than the inactivation produced by a single pulse. Note the "cross-over" of currents for long versus repeated pulses in Fig. 4, *A* and *B*. That is to be expected, as some channels may recover from inactivation during the period at −90 mV between pulses. The interaction of inactivation (at +80 mV) and recovery (at −90 mV) could

explain the faster time constant with repetitive pulses, but recovery from inactivation would tend to reduce the amount of inactivation at all times, in contrast to the observed excessive cumulative inactivation. (Cumulative inactivation was stronger with interpulse intervals at −40 or −60 mV; data not shown.)

In 60 mM K_o^+, repeated pulses also produced excessive cumulative inactivation, but the steady-state levels were lower than with 5 mM K_o^+. That is also expected, because the main effect of high K_o^+ was to speed recovery from inactivation (Fig. 3 *C*).

An allosteric model for inactivation of Kv2.1

A model for inactivation of Kv2.1 should be able to explain the following key features of our data. The voltage-dependence for inactivation is U-shaped, at maximum near the voltage producing half activation, with considerable inactivation at voltages where few channels open. There is excessive cumulative inactivation during repetitive pulses. Development of inactivation has a slight, U-shaped voltage dependence, whereas recovery from inactivation is strongly voltage-dependent, and can be rapid.

Our starting point was the idea that inactivation occurs preferentially from "partially activated" closed states. (By
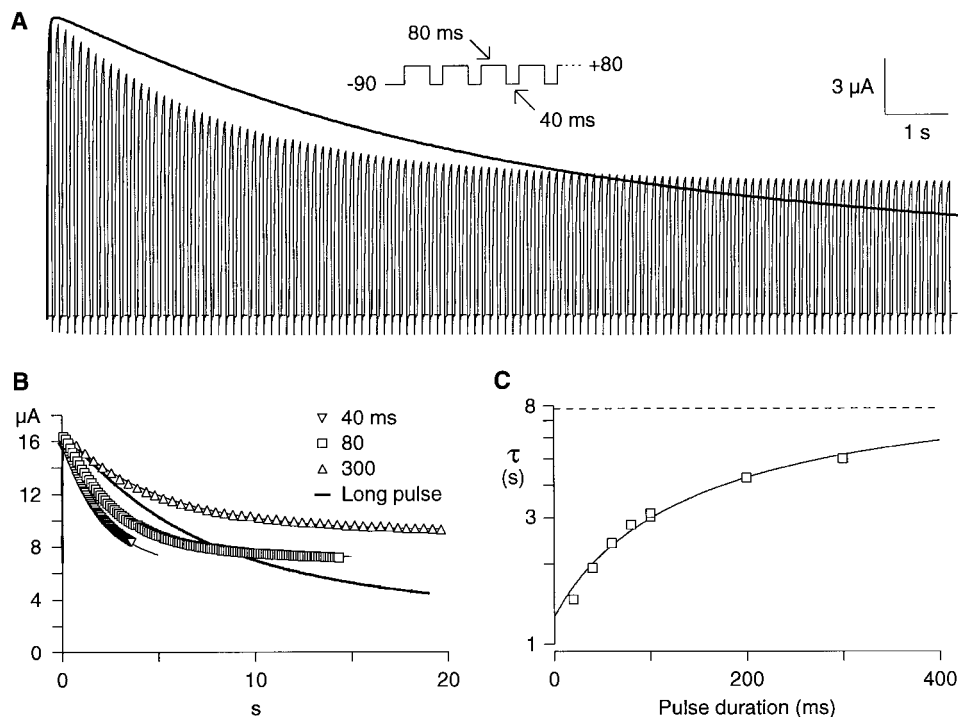

FIGURE 4   Cumulative inactivation. (*A*) Inactivation was compared for a single long pulse from the holding potential of −90 mV to +80 mV (continuous record), versus repeated pulses (80 ms at +80 mV alternating with 40 ms at −90 mV; see diagram of protocol). (*B*) The rate of cumulative inactivation depended on pulse duration. The time course of inactivation was measured from the peak current for each pulse (*symbols*) and for inactivation during a single long pulse to +80 mV (*continuous trace*). For repeated pulses, the duty cycle was 2:1, e.g., for 300-ms pulses, each repolarization to −90 mV lasted 150 ms. Curves drawn through the data are single exponential fits. Both here and in part *A*, the repeated currents were scaled to the amplitude of the current during the long pulse, measured at the time when the first repeated pulse ended. (*C*) Time constants for inactivation during repeated pulses, as a function of pulse duration, for data including that shown in *B*, on a semilogarithmic scale. The dashed line is the time constant for inactivation during a long pulse.

A

B
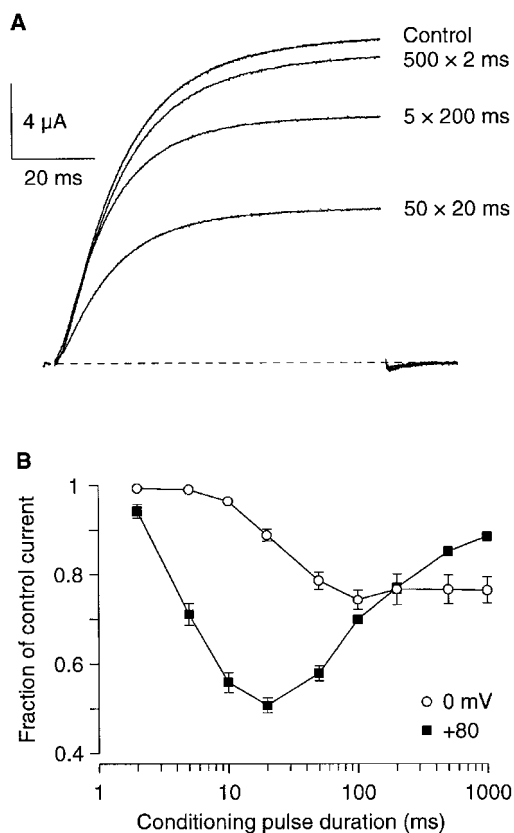
FIGURE 5   Effect of pulse length on inactivation. The number of pulses was varied to give a total of 1 s of depolarization for each pulse length. Interpulse intervals were 50 ms, at the holding potential of -90 mV. After each train, after a delay of 50 ms, a single 80-ms test pulse was given to $+80$ mV to measure the extent of inactivation caused by the train. Cells were held at -90 mV for 30 s between trains, or before giving control test pulses. (*A*) Sample records of test pulses from one cell. The records (in the order recorded) were 1) control; 2) after a train of 500 pulses to $+80$ mV, each lasting 2 ms; 3) after 50 20-ms pulses to $+80$ mV; 4) after five 200-ms pulses to $+80$ mV; and 5) control. Records were leak subtracted, with 1 ms blanked at the start and end of each voltage step. (*B*) Dependence of inactivation on pulse length. Trains of pulses were given to either 0 mV or $+80$ mV. Values are means $\pm$ SEM (shown if larger than the symbol) for seven cells from a single batch of oocytes.

"partially activated" we mean nonconducting states that have some or all voltage sensors in the activated position.) In such a model, both the resting state of the channel and the fully activated open state are protected from inactivation. This can explain the U shape, because more channels are in partially activated states at voltages near the midpoint of the activation curve. It can also explain cumulative inactivation, as channels must pass through partially activated states as they open and close.

We began with a six-state linear model for activation, in which sequential movement of four voltage sensors (as in the original model of Hodgkin and Huxley, 1952) is followed by a concerted channel opening step (Zagotta and Aldrich, 1990; Koren et al., 1990) (*top row of states* in Fig. 6). If the microscopic channel closing step (k_{-O} in Fig. 6) is allowed to depend on voltage, that model can explain many

features of the activation kinetics of the Kv2.1 channel, notably a combination of rapid channel closing at negative voltages with relatively slow and weakly voltage-dependent channel opening at positive voltages (Shieh et al., 1997).

Initially, we tried to simulate inactivation by connecting a single inactivated state to one of the closed states (C_2–C_4). Such models were unable to reproduce the combination of relatively voltage-independent inactivation with voltage-dependent recovery (Fig. 3 *C*). We then turned to a model that naturally produces that result, where microscopic inactivation is independent of voltage, but is allosterically coupled to voltage sensor movement (Jones, 1992; Kuo and Bean, 1994) (Fig. 6). If inactivation from the open state is not allowed ($g = 0$), the addition of inactivation adds only three free parameters to the model: the voltage-independent microscopic inactivation and recovery rates, plus an allosteric factor (f) that determines how strongly inactivation is favored by activation of voltage sensors. Conversely, deactivation of voltage sensors favors recovery from inactivation, producing voltage-dependent recovery.

With $g = 0$ (inactivation only from closed states), the qualitative features of the data were reproduced (not shown). But that model actually gave exaggerated U-shaped voltage dependences for inactivation, and for the time constant of inactivation. We next examined the effect of including inactivation directly from the open state. With $g > 0.1$, the U shape and excessive cumulative inactivation were absent or weak, but a small amount of open-state inactivation ($g = 0.02$) did improve the description of the data.

Fig. 7 *A* shows currents simulated with the model (Fig. 6) for the protocol of Fig. 2 *B*. Both the extent (Fig. 7 *B*) and rate (Fig. 7 *C*) of inactivation have a U-shaped voltage dependence. That U-shaped voltage dependence arises from preferential inactivation from closed states, especially because the C_4–O_4 step favors O_4 for strong depolarization. (For the parameters used here, inactivation occurs mainly from the C_4 state. Even during maintained depolarizations, more channels inactivate via $O_4 \rightarrow C_4 \rightarrow I_4$ than directly from O_4.) The voltage dependence of recovery from inactivation is also well reproduced (Fig. 7 *C*). Repeated pulses produce excessive cumulative inactivation (Fig. 7 *D*). When the pulse length was varied, the extent of inactivation (Fig. 7 *E*) paralleled the occupancy of the C_4 state (Fig. 7 *F*), depending nonmonotonically on pulse length at $+80$ mV but not at 0 mV. In contrast, occupancy of O_4 increased monotonically with pulse length (not shown).

DISCUSSION

Inactivation of Kv2.1 exhibits two features that have rarely been reported for K$^+$ channels: a U-shaped voltage dependence and excessive cumulative inactivation. We propose that these properties can be explained by preferential inactivation from "partially activated" closed states. Occupancy of such closed states can be maximized either at intermediate voltages (producing the U shape) or by repetitive pulses
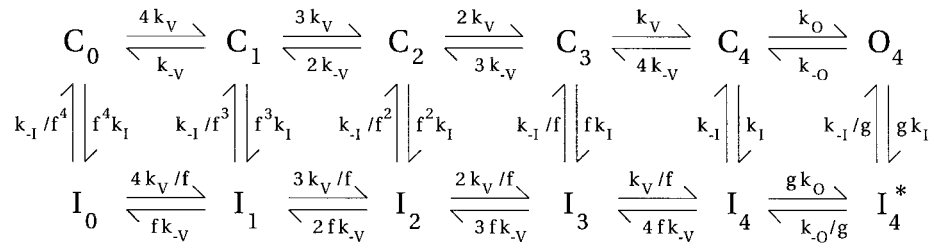
$$C_0 \underset{k_{-V}}{\overset{4k_V}{\rightleftharpoons}} C_1 \underset{2k_{-V}}{\overset{3k_V}{\rightleftharpoons}} C_2 \underset{3k_{-V}}{\overset{2k_V}{\rightleftharpoons}} C_3 \underset{4k_{-V}}{\overset{k_V}{\rightleftharpoons}} C_4 \underset{k_{-O}}{\overset{k_O}{\rightleftharpoons}} O_4$$

$$\begin{array}{cccccc} k_{-I}/f^4 \big\updownarrow f^4 k_I & k_{-I}/f^3 \big\updownarrow f^3 k_I & k_{-I}/f^2 \big\updownarrow f^2 k_I & k_{-I}/f \big\updownarrow f k_I & k_{-I} \big\updownarrow k_I & k_{-I}/g \big\updownarrow g k_I \end{array}$$

$$I_0 \underset{fk_{-V}}{\overset{4k_V/f}{\rightleftharpoons}} I_1 \underset{2fk_{-V}}{\overset{3k_V/f}{\rightleftharpoons}} I_2 \underset{3fk_{-V}}{\overset{2k_V/f}{\rightleftharpoons}} I_3 \underset{4fk_{-V}}{\overset{k_V/f}{\rightleftharpoons}} I_4 \underset{k_{-O}/g}{\overset{gk_O}{\rightleftharpoons}} I_4^*$$

FIGURE 6   An allosteric model for inactivation of Kv2.1. The rate constants for voltage sensor movement at 0 mV (s^{-1}) were $k_V = 121$ and $k_{-V} = 42$; the rate constants for channel opening and closing at 0 mV were $k_O = 80$ and $k_{-O} = 31$; the rate constants for inactivation and recovery (with all voltage sensors activated) were $k_I = 1.2$ and $k_{-I} = 0.005$; and the apparent charge associated was $z = 0.77$ for k_V, $z = -0.54$ for k_{-V}, and $z = -0.50$ for k_{-O}. The rate constants k_O, k_I, and k_{-I} were independent of voltage; others depended exponentially on voltage. The allosteric factors $f = 0.17$ and $g = 0.02$. The model includes 11 free parameters: six rate constants at 0 mV, three voltage dependences, and the two allosteric factors.

that repeatedly cycle the channel through the intermediate closed states (leading to excessive cumulative inactivation). We consider below the experimental precedents for these observations, the proposed model, and other possible explanations for our results.

Key features of delayed rectifier inactivation

We distinguish simple cumulative inactivation, in which the peak current during a pulse is less than at the end of a preceding pulse, from excessive cumulative inactivation, in which a train of pulses produces more inactivation than a single pulse of the same duration. Cumulative inactivation is a common feature of K$^+$ channel inactivation, for both A-current (Furukawa, 1995) and delayed rectifiers. However, we are aware of only two previous reports of excessive cumulative inactivation, for K$^+$ currents of molluscan neurons (Neher and Lux, 1971; Ma and Koester, 1996).

Inactivation increases monotonically with depolarization for Kv1.3 in lymphocytes (Cahalan et al., 1985) and for *Shaker* (Hoshi et al., 1991). However, U-shaped inactivation curves have been reported previously for K$^+$ currents in molluscan neurons (Aldrich et al., 1979a) and for N-terminal-deleted Kv1.4 (Rasmusson et al., 1995a). Hints of the phenomenon exist in published records for Kv2.1 (VanDongen et al., 1990; Pak et al., 1991). However, there seems to have been no previous explanation for U-shaped inactivation of K$^+$ channels.

U-shaped voltage dependence is most famous as an indicator of Ca^{2+}-dependent inactivation of Ca^{2+} channels (Eckert and Chad, 1984). However, a U shape has also been observed for N-type Ca^{2+} channels, under conditions where inactivation was not Ca^{2+}- or current-dependent by other criteria (Jones and Marks, 1989). U-shaped inactivation also occurs for some Na$^+$ channels (Chandler and Meves, 1970). This seems to be a common, although not ubiquitous, feature of "voltage-dependent" inactivation of Ca^{2+}, Na$^+$, and now K$^+$ channels. It will be interesting to determine whether U-shaped inactivation curves also reflect closed-state inactivation for these other channels.

Recovery from inactivation is often very slow for Kv1 channels, much slower than the development of inactivation

(Cahalan et al., 1985; Hoshi et al., 1991; Levy and Deutsch, 1996). In contrast, for Kv2.1, the time constant for recovery from inactivation can be >10-fold faster than the 4–7-s time constant for development of inactivation. This need not reflect fundamental differences between inactivation mechanisms in Kv1 and Kv2.1 channels. If the voltage dependence of recovery results from kinetic coupling to the activation process, slow deactivation (as observed for Kv1.3; Cahalan et al., 1985; Marom and Levitan, 1994) would lead to slow recovery from inactivation. Some delayed rectifier K$^+$ channels do recover fairly rapidly from inactivation, including those in squid axon (Chabala, 1984) and thalamic relay neurons (Huguenard and Prince, 1991).

In *Shaker* and Kv1.3 K$^+$ channels, "C-type" inactivation is slowed by extracellular TEA or K$^+$, reflecting occupancy of a binding site near the extracellular side of the pore (Grissmer and Cahalan, 1989; Choi et al., 1991; López-Barneo et al., 1993). These phenomena were not observed for Kv2.1, where inactivation was actually slightly faster in high K$_o^+$ (Fig. 3 *C*). It is possible that in Kv2.1 occupancy of the crucial binding site is maintained by K$_i^+$ ions permeating the channel (Baukrowitz and Yellen, 1996). However, effects of TEA$_o$ and K$_o^+$ can vary. TEA$_o$ also had no effect on the inactivation of *Aplysia Shab* channels (Quattrocki et al., 1994). In addition, Kv1.3 with a H399Y mutation exhibits faster rather than slower inactivation in the presence of TEA$_o$ or K$_o^+$ (Panyi and Deutsch, 1997). Strikingly, the corresponding residue in Kv2.1 is a tyrosine (the final Y in the sequence GYGDIY). One interpretation is that the effect of TEA$_o$ or K$_o^+$ is not a direct physical interference with inactivation, but an allosteric effect that can be either positive or negative, depending on the pore structure.

In summary, the main results reported here are excessive cumulative inactivation, U-shaped voltage dependence of inactivation, rapid voltage-dependent recovery from inactivation, and weak effects of TEA$_o$ and K$_o^+$ on development of inactivation. Although there is some precedent for each of these results, they are not standard or well-established general properties of delayed rectifiers. As discussed above, it is not clear whether these differences imply that inactivation of Kv2.1 is fundamentally different from C-type inactivation of Kv1 channels. Further studies will be nec-
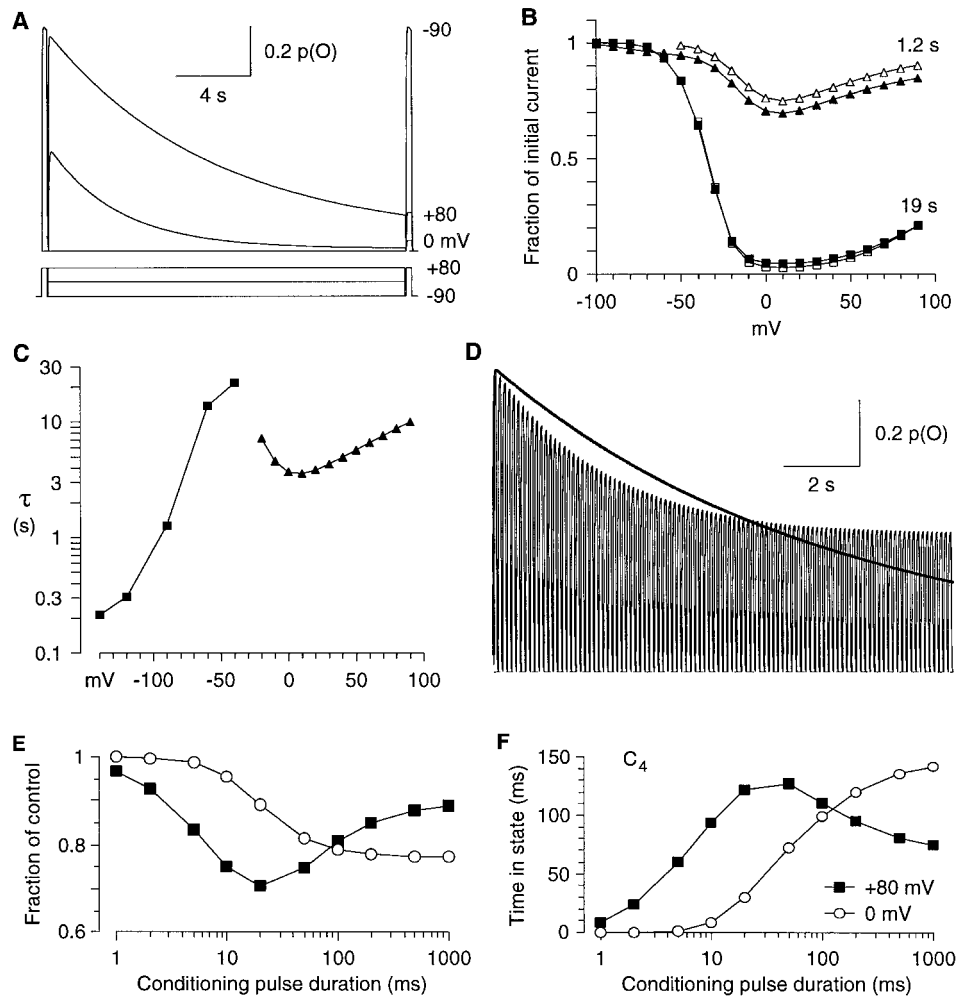
FIGURE 7   Simulation of the allosteric model for inactivation. Parameters are given in Fig. 6. (*A*) Inactivation, simulated with the protocol of Fig. 2 *B*. (*B*) The voltage dependence of inactivation, as measured from the I3/I1 ratio (▲, ■), or the I2(end)/I2(peak) ratio (△, □). Simulations used middle pulses lasting 1.2 s (△, ▲) or 19 s (■, □). (*C*) The voltage dependence of time constants for inactivation (▲) and recovery (■), for the model using the protocols of Figs. 2–3. (*D*) Excessive cumulative inactivation. Pulses were given to +80 mV for 80 ms, with interpulse intervals of 40 ms at −90 mV. The continuous record, in units of *p*(open), with peak *p*(open) = 0.9, is for a maintained depolarization to +80 mV. (*E*) Simulation of the effect of pulse length on inactivation. Each train of pulses included a total of 1 s of depolarization, by the protocol of Fig. 5. Pulses were to 0 mV (○) or +80 mV (■). (*F*) Occupancy of the C_4 state, for the simulations in *E*. The vertical axis is the total amount of time spent in the C_4 state during the protocol, including both the pulses themselves and the interpulse intervals. The initial increase in inactivation with pulse length (up to 20 ms) reflects both increased occupancy of C_4 and decreased recovery from inactivation (with short pulse lengths, there are more interpulse intervals, and thus there is more recovery from inactivation between pulses).

essary, notably testing for excessive cumulative inactivation in other delayed rectifiers. We do have preliminary evidence for a U-shaped voltage dependence of inactivation, and excessive cumulative inactivation, for the delayed rectifier K^+ current of frog sympathetic neurons (J. Xie, K. G. Klemic, and S. W. Jones, unpublished observations). The observation of those phenomena for a native channel argues that they do not result from aberrant behavior of Kv2.1 expressed in oocytes.

Models for cumulative inactivation

Cumulative inactivation is often taken to mean that channels continue to inactivate in the interpulse interval. That would

not occur with a Hodgkin and Huxley (1952) model, in which inactivation depends on voltage rather than on the state of the channel. Continued inactivation "on the way down" could occur either from the open state (DeCoursey, 1990; Lee and Deutsch, 1990), or from a closed state that is closely linked kinetically to the open state (Marom and Levitan, 1994). However, inactivation can also occur "on the way up," between the beginning of the depolarization and peak activation. That is the predominant pathway in the model of Aldrich (1981). Surprisingly, cumulative inactivation "on the way up" can also occur with purely voltage-dependent inactivation. We find that the Hodgkin and Huxley (1952) model generates cumulative inactivation for trains of brief depolarizations (e.g., 0.5 ms pulses to +20

mV; not shown). Because inactivation is equally fast from closed and open states, a considerable fraction of channels inactivate before opening. Thus cumulative inactivation appears to be a somewhat counterintuitive consequence of a variety of models for inactivation, as long as recovery from inactivation at the holding potential is relatively slow. Excessive cumulative inactivation may be more useful for distinguishing models. At the least, it seems incompatible with purely voltage-dependent inactivation.

Cumulative inactivation is often associated with slow channel closing, where inactivation between the end of one pulse and the peak of the next presumably occurs "on the way down" (DeCoursey, 1990; Lee and Deutsch, 1990). However, deactivation of Kv2.1 is fast ($\tau = 5$ ms at -90 mV), especially compared to activation ($\tau = 12$ ms at $+80$ mV; Shieh et al., 1997; K. G. Klemic, unpublished observations). This is more consistent with inactivation that occurs predominantly "on the way up." In terms of our proposed model, the channel spends more time in the crucial C_4 state during the activation process, because the voltage-independent $C_4 \rightarrow O_4$ transition is rate-limiting, whereas $C_4 \rightarrow C_3$ is fast at negative voltages.

A phenomenon often associated with cumulative inactivation of K^+ channels is a U-shaped or biphasic time course of recovery from inactivation (Neher and Lux, 1971; Aldrich et al., 1979a; Marom and Levitan, 1994), where lengthening the interpulse interval initially increases the amount of inactivation. That effect is also observed for Kv2.1 (and for our model; not shown), when the initial pulse is brief and causes little inactivation, even though monoexponential recovery is observed after long pulses (Fig. 3). We have not examined this effect in detail, because it is expected both for open- or closed-channel inactivation. In addition, apparent biphasic recovery from inactivation is observed even for the Hodgkin-Huxley Na^+ channel model, although in that case the initial decrease in test pulse current with increasing interpulse interval reflects channel closing, rather than a true increase in inactivation (Gillespie and Meves, 1980).

Allosteric model for inactivation

The kinetic model that we propose (Fig. 6) is based on the classic Monod–Wyman–Changeux model (Monod et al., 1965) for activation of allosteric proteins such as hemoglobin. It is attractive to assume that ion channels are analogous to other allosteric proteins (Patlak, 1991; Hille, 1992), because multiple subunits (or domains) must cooperate in the regulation of a single pore. MWC models have been proposed previously for both activation (Marks and Jones, 1992; McCormack et al., 1994) and inactivation (Jones, 1992; Kuo and Bean, 1994) of voltage-dependent channels. The fundamental idea is that activation of a voltage sensor, e.g., a local conformational change in one S4 region, stabilizes the open (or inactivated) state of the channel by a fixed amount of energy. Allosteric coupling of activation to in-

activation is also in the spirit of the Armstrong and Bezanilla (1977) model for Na^+ channel inactivation.

The model used here has the same form as that of Kuo and Bean (1994), but our parameters produce weak inactivation from the open state of the channel. It is not difficult to picture how channel opening could affect an inactivation process, either positively or negatively. Either the conformational change involved in channel opening, or the presence of ions permeating the pore, could affect the rate of inactivation from the open state. It is noteworthy that Kuo and Bean (1994) used open state inactivation primarily to explain a delay in recovery from inactivation for Na^+ channels, which we have not observed for the Kv2.1 K^+ channel (Fig. 3 B). It is possible that open state inactivation will be more important for other K^+ channels or for channel mutants (De Biasi et al., 1993).

C-type inactivation of K^+ channels is believed to be a concerted process involving constriction of the outer mouth of the pore (Liu et al., 1996). This fits nicely with an allosteric model. It is interesting, however, that the model can also describe inactivation of Na^+ channels (Kuo and Bean, 1994). Na^+ channel inactivation is believed to resemble N-type inactivation, because both result from binding of an intracellular domain of the channel to a site near the inner mouth of the pore. It is plausible that either N- or C-type inactivation, either binding or a concerted conformational change, could be coupled allosterically to voltage sensor movement. Such a model is worth considering for any inactivation process in which development of inactivation is weakly voltage-dependent (reflecting the voltage-independent microscopic inactivation rates), but recovery is strongly voltage-dependent (reflecting coupling of activation to inactivation). However, recovery from inactivation tends to occur via closed states in the model, so other schemes might be preferable when there is evidence for recovery through the open state (e.g., N-type inactivation of *Shaker*: Demo and Yellen, 1991; Ruppersberg et al., 1991).

Of course, it is possible that other models could explain our results. For N-type Ca^{2+} channels, a U-shaped inactivation curve was explained by a cyclic C-O-I model, in which microscopic inactivation was actually favored by hyperpolarization (Jones and Marks, 1989). That model does predict cumulative inactivation, but shows excessive cumulative inactivation only if significant inactivation occurs from the closed state. It also postulates an intrinsic voltage sensor specific to the inactivation process, which is not necessary with the allosteric model.

With another model, suggested by one of the reviewers, inactivation occurs from an open state, but a second open state (populated at positive voltages and/or long depolarizations) cannot inactivate (see also Chandler and Meves, 1970; Armstrong and Bezanilla, 1977). That model can produce excessive cumulative inactivation and a U-shaped voltage dependence of inactivation. This demonstrates that closed state inactivation is not absolutely necessary to explain these phenomena, although protection of an open state from inactivation may be required. For Kv2.1, we are re-

luctant to adopt a model that depends on the existence of two open states, because single-channel open times are exponentially distributed (Shieh et al., 1997), as commonly observed for Kv channels (Hoshi et al., 1994).

With the allosteric model, at most voltages, inactivation occurs primarily from the closed state with all four voltage sensors activated (C_4). Our data do not rule out the possibility of preferential inactivation from C_2 and/or C_3, but such a model would require additional free parameters.

Another possibility is that the inactivation reported here, or some component of it, actually results from voltage-dependent block by an intracellular cation. To explain the decreased inactivation at positive voltages, the voltage dependence must be the reverse of that normally observed for block by an intracellular cation, but that could occur if the blocker is able to permeate at strongly depolarized voltages. Block with at least some of these properties has been reported for intracellular 4-aminopyridine (Rasmusson et al., 1995b). We cannot completely exclude this possibility, but preliminary experiments with inside-out patches from oocytes suggest that inactivation does not "wash out," but rather becomes stronger, although that effect is difficult to distinguish from rundown.

In summary, the model (Fig. 6) is one relatively simple explanation of the qualitative features of our data. We do not claim that the model is unique, or that it is a complete description of gating of Kv2.1 channels. In addition, further work will be necessary to determine whether the model is applicable to inactivation of other voltage-dependent channels, including slow inactivation of other K^+ channels.

Physiological significance of closed state inactivation

Because K^+ channel inactivation is accelerated by repetitive depolarization, it is possible that cumulative inactivation could occur during a train of action potentials (Aldrich et al., 1979b; Ma and Koester, 1996). In our experiments, cumulative inactivation was still rather slow ($\tau \sim 1$ s for the most rapid pulses tested), but it should be recognized that these experiments were conducted at room temperature. Heterologous expression of Kv2.1 channels in *Xenopus* oocytes is useful for the establishment of biophysical mechanisms, but clearly this is not an appropriate system for testing the physiological role of cumulative inactivation.

The voltage dependence of recovery may also be important. Recovery from inactivation should be relatively fast at the resting potential, and even faster during an afterhyperpolarization. However, neurons often fire bursts of action potentials with a relatively depolarized interspike voltage, which seems ideally designed to maximize cumulative inactivation. This mechanism may contribute to the commonly observed broadening of action potentials during a burst (Aldrich et al., 1979b; Ma and Koester, 1996). Finally, acceleration of recovery from inactivation by K_o^+ could limit K^+ channel inactivation during periods of intense activity. Further study of delayed rectifier K^+ channels in neurons will be necessary to test these ideas.

REFERENCES

Aldrich, R. W. 1981. Inactivation of voltage-gated delayed potassium current in molluscan neurons. A kinetic model. *Biophys. J.* 36:519–532.

Aldrich, R. W., P. A. Getting, and S. H. Thompson. 1979a. Inactivation of delayed outward current in molluscan neurone somata. *J. Physiol. (Lond.).* 291:507–530.

Aldrich, R. W., P. A. Getting, and S. H. Thompson. 1979b. Mechanism of frequency-dependent broadening of molluscan neurone soma spikes. *J. Physiol. (Lond.).* 291:531–544.

Armstrong, C. M., and F. Bezanilla. 1977. Inactivation of the sodium channel. II. Gating current experiments. *J. Gen. Physiol.* 70:567–590.

Barry, D. M., J. S. Trimmer, J. P. Merlie, and J. M. Nerbonne. 1995. Differential expression of voltage-gated K^+ channel subunits in adult rat heart. Relation to functional K^+ channels? *Circ. Res.* 77:361–369.

Baukrowitz, T., and G. Yellen. 1996. Use-dependent blockers and exit rate of the last ion from the multi-ion pore of a K^+ channel. *Science.* 271:653–656.

Brahmajothi, M. V., M. J. Morales, S. Liu, R. L. Rasmusson, D. L. Campbell, and H. C. Strauss. 1996. In situ hybridization reveals extensive diversity of K^+ channel mRNA in isolated ferret cardiac myocytes. *Circ. Res.* 78:1083–1089.

Cahalan, M. D., K. D. Chandy, T. E. DeCoursey, and S. Gupta. 1985. A voltage-gated potassium channel in human T lymphocytes. *J. Physiol. (Lond.).* 358:197–237.

Chabala, L. D. 1984. The kinetics of recovery and development of potassium channel inactivation in perfused squid (*Loligo pealei*) giant axons. *J. Physiol. (Lond.).* 356:193–220.

Chandler, W. K., and H. Meves. 1970. Evidence for two types of sodium conductance in axons perfused with sodium fluoride solution. *J. Physiol. (Lond.).* 211:653–678.

Choi, K. L., R. W. Aldrich, and G. Yellen. 1991. Tetraethylammonium blockade distinguishes two inactivation mechanisms in voltage-activated K^+ channels. *Proc. Natl. Acad. Sci. USA.* 88:5092–5095.

De Biasi, M., H. A. Hartmann, J. A. Drewe, M. Taglialatela, A. M. Brown, and G. E. Kirsch. 1993. Inactivation determined by a single site in K^+ pores. *Pflügers Arch.* 422:354–363.

DeCoursey, T. E. 1990. State-dependent inactivation of K^+ currents in rat type II alveolar epithelial cells. *J. Gen. Physiol.* 95:617–649.

DeCoursey, T. E., K. G. Chandy, S. Gupta, and M. D. Cahalan. 1984. Voltage-gated K^+ channels in human T lymphocytes: a role in mitogenesis? *Nature.* 307:465–468.

Demo, S. D., and G. Yellen. 1991. The inactivation gate of the *Shaker* K^+ channel behaves like an open-channel blocker. *Neuron.* 7:743–753.

Dixon, J. E., and D. McKinnon. 1994. Quantitative analysis of potassium channel mRNA expression in atrial and ventricular muscle of rats. *Circ. Res.* 75:252–260.

Dixon, J. E., and D. McKinnon. 1996. Potassium channel mRNA expression in prevertebral and paravertebral sympathetic neurons. *Eur. J. Neurosci.* 8:183–191.

Drewe, J. A., H. A. Hartmann, and G. E. Kirsch. 1994. K^+ channels in mammalian brain: a molecular approach. *Methods Neurosci.* 19: 243–260.

Drewe, J. A., S. Verma, G. Fresch, and R. H. Joho. 1992. Distinct spatial and temporal expression patterns of K^+ channel mRNAs from different subfamilies. *J. Neurosci.* 12:538–548.

Eckert, R., and J. E. Chad. 1984. Inactivation of Ca channels. *Prog. Biophys. Mol. Biol.* 44:215–267.

Frech, G. C., A. M. J. VanDongen, G. Schuster, A. M. Brown, and R. H. Joho. 1989. A novel potassium channel with delayed rectifier properties isolated from rat brain by expression cloning. *Nature.* 340:642–645.

Furukawa, Y. 1995. Accumulation of inactivation in a cloned transient K^+ channel (AKv1.1a) of *Aplysia. J. Neurophysiol.* 74:1248–1257.

Gillespie, J. I., and H. Meves. 1980. The time course of sodium inactivation in squid giant axons. *J. Physiol. (Lond.).* 299:389–307.

Grissmer, S., and M. Cahalan. 1989. TEA prevents inactivation while blocking open K^+ channels in human T lymphocytes. *Biophys. J.* 55:203–206.

Hille, B. 1992. Ionic Channels of Excitable Membranes, 2nd Ed. Sinauer Associates, Sunderland, MA.

Hodgkin, A. L., and A. F. Huxley. 1952. A quantitative description of membrane current and its application to conduction and excitation in nerve. *J. Physiol.* 117:500–544.

Hoshi, T., W. N. Zagotta, and R. W. Aldrich. 1990. Biophysical and molecular mechanisms of Shaker potassium channel inactivation. *Science.* 250:533–538.

Hoshi, T., W. N. Zagotta, and R. W. Aldrich. 1991. Two types of inactivation of Shaker K^+ channels: effects of alterations in the carboxy-terminal region. *Neuron.* 7:547–556.

Hoshi, T., W. N. Zagotta, and R. W. Aldrich. 1994. *Shaker* potassium channel gating. I. Transitions near the open state. *J. Gen. Physiol.* 103:249–278.

Huguenard, J. R., and D. A. Prince. 1991. Slow inactivation of a TEA-sensitive K current in acutely isolated rat thalamic relay neurons. *J. Neurophysiol.* 66:1316–1328.

Ikeda, S. R., F. Soler, R. D. Zühlke, R. H. Joho, and D. L. Lewis. 1992. Heterologous expression of the human potassium channel Kv2.1 in clonal mammalian cells by direct cytoplasmic microinjection of cRNA. *Pflügers Arch.* 422:201–203.

Jones, S. W. 1992. An allosteric model for inactivation of voltage-dependent channels. *Soc. Neurosci. Abstr.* 18:973.

Jones, S. W., and T. N. Marks. 1989. Calcium currents in bullfrog sympathetic neurons. II. Inactivation. *J. Gen. Physiol.* 94:169–182.

Klemic, K. G., C.-C. Shieh, G. E. Kirsch, and S. W. Jones. 1997. Gating kinetics of the rat Kv2.1 potassium channel expressed in *Xenopus* oocytes. *Biophys. J.* 72:A27 (Abstr.).

Koren, G., E. R. Liman, D. E. Logothetis, B. Nadal-Ginard, and P. Hess. 1990. Gating mechanism of a cloned potassium channel expressed in frog oocytes and mammalian cells. *Neuron.* 4:39–51.

Kuo, C.-C., and B. P. Bean. 1994. Na^+ channels must deactivate to recover from inactivation. *Neuron.* 12:819–829.

Lee, S. C., and C. Deutsch. 1990. Temperature dependence of K^+-channel properties in human T lymphocytes. *Biophys. J.* 57:49–62.

Levy, D. I., and C. Deutsch. 1996. Recovery from C-type inactivation is modulated by extracellular potassium. *Biophys. J.* 70:798–805.

Liu, Y., M. E. Jurman, and G. Yellen. 1996. Dynamic rearrangement of the outer mouth of a K^+ channel during gating. *Neuron.* 16:859–867.

López-Barneo, J., T. Hoshi, S. H. Heinemann, and R. W. Aldrich. 1993. Effects of external cations and mutations in the pore region on C-type inactivation of *Shaker* potassium channels. *Receptors Channels.* 1:61–71.

Ma, M., and J. Koester. 1996. The role of K^+ currents in frequency-dependent spike broadening in *Aplysia* R20 neurons: a dynamic-clamp analysis. *J. Neurosci.* 16:4089–4101.

Marks, T. N., and S. W. Jones. 1992. Calcium currents in the A7r5 smooth muscle-derived cell line. An allosteric model for calcium channel activation and dihydropyridine agonist action. *J. Gen. Physiol.* 99:367–390.

Marom, S., S. A. N. Goldstein, J. Kupper, and I. B. Levitan. 1993. Mechanism and modulation of inactivation of the Kv3 potassium channel. *Receptors Channels.* 1:81–88.

Marom, S., and I. B. Levitan. 1994. State-dependent inactivation of the Kv3 potassium channel. *Biophys. J.* 67:579–589.

Mathes, C., J. J. C. Rosenthal, C. M. Armstrong, and W. F. Gilly. 1997. Fast inactivation of delayed rectifier K conductance in squid giant axon and its cell bodies. *J. Gen. Physiol.* 109:435–448.

Matteson, D. R., and C. Deutsch. 1984. K channels in T lymphocytes: a patch clamp study using monoclonal antibody adhesion. *Nature.* 307:468–471.

McCormack, K., W. J. Joiner, and S. H. Heinemann. 1994. A characterization of the activating structural rearrangements in voltage-dependent *Shaker* K^+ channels. *Neuron.* 12:301–315.

Monod, J., J. Wyman, and J.-P. Changeux. 1965. On the nature of allosteric transitions: a plausible model. *J. Mol. Biol.* 12:88–118.

Neher, E., and H. D. Lux. 1971. Properties of somatic membrane patches of snail neurones under voltage clamp. *Pflügers Arch.* 322:35–38.

Ogielska, E. M., W. N. Zagotta, T. Hoshi, S. H. Heinemann, J. Haab, and R. W. Aldrich. 1995. Cooperative subunit interactions in C-type inactivation of K channels. *Biophys. J.* 69:2449–2457.

Pak, M. D., M. Covarrubias, A. Ratcliffe, and L. Salkoff. 1991. A mouse brain homolog of the *Drosophila* Shab K^+ channel with conserved delayed-rectifier properties. *J. Neurosci.* 11:869–880.

Panyi, G., and C. Deutsch. 1997. Anomalous inactivation of a Kv1.3 mutant. *Biophys. J.* 72:A27 (Abstr.).

Panyi, G., Z. Sheng, L. Tu, and C. Deutsch. 1995. C-type inactivation of a voltage-gated K^+ channel occurs by a cooperative mechanism. *Biophys. J.* 69:896–903.

Patlak, J. 1991. Molecular kinetics of voltage-dependent Na^+ channels. *Physiol. Rev.* 71:1047–1080.

Quattrocki, E. A., J. Marshall, and L. K. Kaczmarek. 1994. A *Shab* potassium channel contributes to action potential broadening in peptidergic neurons. *Neuron.* 12:73–86.

Rasmusson, R. L., M. J. Morales, R. C. Castellino, Y. Zhang, D. L. Campbell, and H. C. Strauss. 1995a. C-type inactivation controls recovery in a fast inactivating cardiac K^+ channel (Kv1.4) expressed in *Xenopus* oocytes. *J. Physiol. (Lond.).* 489:709–721.

Rasmusson, R. L., Y. Zhang, D. L. Campbell, M. B. Comer, R. C. Castellino, S. Liu, S., and H. L. Strauss. 1995b. Bi-stable block by 4-aminopyridine of a transient K^+ channel (Kv1.4) cloned from ferret ventricle and expressed in *Xenopus* oocytes. *J. Physiol. (Lond.).* 485:59–71.

Ruppersberg, J. P., R. Frank, O. Pongs, and M. Stocker. 1991. Cloned neuronal $I_K(A)$ channels reopen during recovery from inactivation. *Nature.* 353:657–660.

Schreibmayer, W., H. A. Lester, and N. Dascal. 1994. Voltage clamping of *Xenopus laevis* oocytes utilizing agarose-cushion electrodes. *Pflügers Arch.* 426:453–458.

Shi, G., A. K. Kleinklaus, N. V. Marrion, and J. S. Trimmer. 1994. Properties of Kv2.1 K channels expressed in transfected mammalian cells. *J. Biol. Chem.* 269:23204–23211.

Shieh, C.-C., K. G. Klemic, and G. E. Kirsch. 1997. Role of transmembrane segment S5 in gating of voltage-dependent K^+ channels. *J. Gen. Physiol.* 109:767–778.

Tillotson, D. 1979. Inactivation of Ca conductance dependent on entry of Ca ions in molluscan neurons. *Proc. Natl. Acad. Sci. USA.* 76:1497–1500.

Trimmer, J. S. 1993. Expression of Kv2.1 delayed rectifier K^+ channel isoforms in the developing rat brain. *FEBS Lett.* 324:205–210.

VanDongen, A. M. J., G. C. Frech, J. A. Drewe, R. H. Joho, and A. M. Brown. 1990. Alteration and restoration of K^+ channel function by deletions at the N- and C-termini. *Neuron.* 5:433–443.

Zagotta, W. N., and R. W. Aldrich. 1990. Voltage-dependent gating of *Shaker* A-type potassium channels in *Drosophila* muscle. *J. Gen. Physiol.* 95:29–60.